



**HAL**  
open science

## **El Niño as a predictor of round sardinella distribution along the northwest African coast**

Jorge López-Parages, Pierre-Amaël Auger, Belén Rodríguez-Fonseca, Noel Keenlyside, Carlo Gaetan, Angelo Rubino, Maeregu Woldeyes Arisido, Timothée Brochier

### ► To cite this version:

Jorge López-Parages, Pierre-Amaël Auger, Belén Rodríguez-Fonseca, Noel Keenlyside, Carlo Gaetan, et al.. El Niño as a predictor of round sardinella distribution along the northwest African coast. *Progress in Oceanography*, 2020, 186, <10.1016/j.pocean.2020.102341>. <insu-03683235>

**HAL Id: insu-03683235**

**<https://insu.hal.science/insu-03683235v1>**

Submitted on 19 Sep 2025

HAL is a multi-disciplinary open access archive for the deposit and dissemination of scientific research documents, whether they are published or not. The documents may come from teaching and research institutions in France or abroad, or from public or private research centers.

L'archive ouverte pluridisciplinaire HAL, est destinée au dépôt et à la diffusion de documents scientifiques de niveau recherche, publiés ou non, émanant des établissements d'enseignement et de recherche français ou étrangers, des laboratoires publics ou privés.



Distributed under a Creative Commons CC BY 4.0 - Attribution - International License

# El Niño as a predictor of round sardinella distribution along the northwest African coast

Jorge López-Parages<sup>a,b,f,\*</sup>, Pierre-Amaël Auger<sup>c,d</sup>, Belén Rodríguez-Fonseca<sup>a</sup>, Noel Keenlyside<sup>e</sup>, Carlo Gaetan<sup>b</sup>, Angelo Rubino<sup>b</sup>, Maeregu W. Arisido<sup>b</sup>, Timothée Brochier<sup>g</sup>

<sup>a</sup>*Dpto de Física de la Tierra y Astrofísica, UCM-IGEO, Complutense University of Madrid, Spain*

<sup>b</sup>*Dpto di Scienze Ambientali, Informatica e Statistica, Ca Foscari University of Venice, Italy*

<sup>c</sup>*Instituto Milenio de Oceanografía and Pontificia Universidad Católica de Valparaíso, Valparaíso, Chile*

<sup>d</sup>*Laboratoire d'Océanographie Physique et Spatiale (LOPS), IUEM, Brest University, CNRS, IRD, Ifremer, Brest, France*

<sup>e</sup>*Bjerknes Centre for Climate Research, Univ. of Bergen, Norway*

<sup>f</sup>*CERFACS/CNRS, Climate Modelling and Global Change Team, 42 avenue Gaspard Coriolis, 31057 Toulouse, France*

<sup>g</sup>*Institut de Recherche pour le Développement (IRD), UMMISCO, Sorbonne University, Université Cheikh Anta Diop, Dakar, Senegal*

---

## Abstract

The El Niño Southern Oscillation (ENSO) produces global marine environment conditions that can cause changes in abundance and distribution of distant fish populations worldwide. Understanding mechanisms acting locally on fish population dynamics is crucial to develop forecast skill useful for fisheries management. The present work addresses the role played by ENSO on the round sardinella population biomass and distribution in the central-southern portion of the Canary Current Upwelling System (CCUS). A combined physical-biogeochemical framework is used to understand the climate influence on the hydrodynamical conditions in the study area. Then, an evolutionary individual-based model is used to simulate the round sardinella spatio-temporal biomass variability. According to model experiments, anomalous oceanographic conditions forced by El Niño along the African

---

\*Corresponding author

*Email address:* [jlopez@cerfacs.fr](mailto:jlopez@cerfacs.fr) (Jorge López-Parages)

coast cause anomalies in the latitudinal migration pattern of the species. A robust anomalous increase and decrease of the simulated round sardinella biomass is identified in winter off the Cape Blanc and the Saharan coast region, respectively, in response to El Niño variations. The resultant anomalous pattern is an alteration of the normal migration between the Saharan and the Mauritanian waters. It is primarily explained by the modulating role that El Niño exerts on the currents off Cape Blanc, modifying therefore the normal migration of round sardinella in the search of acceptable temperature conditions. This climate signature can be potentially predicted up to six months in advance based on El Niño conditions in the Pacific.

*Keywords:* El Nino, Sardinella aurita, Coastal upwelling, Dynamical oceanography, Atmospheric sciences

---

## 1. Introduction

### 1.1. The round sardinella in the CCUS

Small pelagic fishes populations in the so-called *Eastern Boundary Upwelling Systems (EBUS)* are particularly sensitive to global climate change and variability (Bakun, 1990, Bakun et al., 2015, Brochier et al., 2013). These systems, moreover, are of special biological and social importance (Fréon et al., 2009), as they jointly contribute to more than 20% of global fish catches and more than 7% of global marine primary production although they only cover approximately 1% of the total ocean surface (Pauly and Christensen, 1995). The socio-economic relevance of fisheries is especially clear for the Canary Current Upwelling System (CCUS) because of its impact on the economies of the northwest African countries (Failler, 2014). This is particularly true in the case of small pelagic fisheries, as they are the main pelagic fisheries in this region in terms of commercial landings ( $\sim 450.000$  tons per year; Braham et al., 2014).

The CCUS is characterized by a marked spatial and seasonal variability (Chavez and Messié, 2009), especially south of Cape Blanc ( $\sim 20^\circ\text{N}$ ; Carr and Kearns, 2003) and north of the Canary Islands ( $\sim 27^\circ\text{N}$ ; Messié and Chavez, 2015), which is associated with the latitudinal migration of the Intertropical Convergence Zone and the accompanying evolution of the Azores high (Wooster et al., 1976). This variability seems to affect the spatial distribution of migratory fish species such as *Sardinella aurita* (Valenciennes, 1847),

24 which is the most abundant small pelagic fish in the Senegalese-Mauritanian  
25 region. This species, usually called round sardinella, undertakes large north-  
26 south migrations over the continental shelf along northwest Africa, with the  
27 area of maximum abundance being located approximately between 11°N and  
28 25°N (Boëly et al., 1978). Data on fishing effort, fish length distribution, and  
29 coastal environmental variability have facilitated recent refinement of scien-  
30 tific understating concerning the details of this migration pattern (Braham  
31 et al., 2014, Corten et al., 2012, 2017). Recently Brochier et al. (2018) sug-  
32 gested that the migration results from 1) an interplay between sea tempera-  
33 ture and food availability conditions which both influence the habitat quality  
34 of round sardinella, and 2) the effect that coastal currents exert on the pas-  
35 sive advection component of round sardinella horizontal movements. These  
36 environmental variables (sea temperature, food availability, and currents)  
37 also exhibit clear year-to-year differences that modify the seasonal cycle of  
38 the CCUS (Benazzouz et al., 2014). However, the mechanisms behind this  
39 interannual variability are not well understood. Disentangling the climate  
40 influences on the alongshore variability of sea temperature, food abundance,  
41 and coastal currents in northwest Africa would shed light on the related re-  
42 sponse of the round sardinella population. This understanding is crucial to  
43 the development of useful prediction tools for the cooperative management  
44 of fish stocks that span political boundaries, and is thus of great importance  
45 to the economy and food security of the countries in this region (Failler, 2014).  
46

### 47 *1.2. Global climate as a forcing of round sardinella in the CCUS*

48 Coastal upwelling involves the offshore transport of surface water and  
49 its replacement by deep, cold and nutrient-rich waters via Ekman dynam-  
50 ics. This is, therefore, a wind-driven process modulated by the intensity of  
51 the alongshore winds (Barton et al., 1998). Thus, the interannual variability  
52 of surface winds blowing southward alters coastal upwelling, which in turn  
53 triggers changes in the ocean mixed-layer temperature, primary productivity,  
54 and currents. Thermodynamic processes forced by the surface winds can also  
55 alter the upper ocean through heat flux exchanges. Both of the aforemen-  
56 tioned mechanisms (dynamical upwelling and thermodynamic heat fluxes)  
57 are therefore related to the variability of the surface winds (Polo et al., 2005)  
58 and have the potential to alter the round sardinella distribution. Thus, the  
59 round sardinella population size and distribution off northwest Africa could  
60 be related to large-scale patterns of climate variability due to their impact

61 on the trade winds blowing in this region (Binet, 1988).

62

63 Understanding the remote responses of fish populations to climate vari-  
64 ations is a long standing concern of major importance and broad scientific  
65 interest (Overland et al., 2010, Báez et al., 2019). In the case of the CCUS,  
66 this issue has been explored in the past, and the results seem to depend on  
67 several factors including the chosen methodology. An example of this is the  
68 relation with the North Atlantic Oscillation (NAO) which is the dominant at-  
69 mospheric variability mode over the North Atlantic in boreal winter (Czaja  
70 et al., 2002, Visbeck et al., 2003). The occurrence of upwelling-favorable  
71 winds along the northwest African coast is strongly related to the location  
72 and strength of the North Atlantic subtropical high (the Azores high) and  
73 hence, to the NAO (Meiners et al., 2010). However, recent studies in the  
74 CCUS suggest a significant correlation between the NAO and the coastal  
75 upwelling intensity when this is derived from the wind stress, but not when  
76 this is constructed from the difference in sea surface temperature (hereinafter  
77 SST) between the coast and the open ocean (Benazzouz et al., 2014, Crop-  
78 per et al., 2014, Narayan et al., 2010). The El Niño-Southern Oscillation  
79 (ENSO) phenomenon, which is the dominant pattern of global climate vari-  
80 ability at interannual timescales, also impacts the tropical North Atlantic  
81 (TNA) through a variety of mechanisms (Giannini et al., 2001, Wang, 2004,  
82 Lee et al., 2008, García-Serrano et al., 2017). However, few works have an-  
83 alyzed the impact of ENSO on the CCUS and, as in the case of NAO, they  
84 conflict on whether a significant signature exists (see e.g., Roy and Reason,  
85 2001 and Oettli et al., 2016). Estimating the local signature of these global  
86 climate modes on round sardinella population in the CCUS is a priori even  
87 harder, as the available abundance data, even with state of the art obser-  
88 vational capabilities, are scarce or of low quality. There are also intrinsic  
89 limitations in round sardinella catch data associated with the difficulty of  
90 distinguishing environmental influences (i.e., not directly related to changes  
91 in human activities) and human-related influences. The second includes vari-  
92 ability of the market demand, changes in fishing gear and fleet composition,  
93 and improvements in fishermen technical skill over time (see e.g., discussion  
94 in Bez and Braham, 2014). The recent and interesting observational analy-  
95 ses of the CCUS (see e.g., Braham et al., 2014) do not clarify the multiple  
96 environmental factors impacting round sardinella spatio-temporal variability.

97

98 New approaches are required to move beyond these conflicting results.

99 Despite their deficiencies, models provide a means to overcome the inherent  
100 limitations of observational analysis. For example, investigation of model  
101 simulations permit researchers to isolate the climate-related responses from  
102 the direct human influence. In the present study, a modeling approach has  
103 been used to investigate the influence of ENSO on the interannual variability  
104 in the biomass and spatial distribution of a simulated round sardinella  
105 population in the central-southern portion of the CCUS.

## 106 **2. Material and methods**

### 107 *2.1. Modeling strategy*

108 The study region (hereinafter referred as CCUS; see Fig. 1) is the upper  
109 ocean east of 24°W and between 10°N and 35°N. This geographic area is  
110 divided in three distinct regions according to the intensity and seasonal variability  
111 of upwelling-favorable winds: the Mauritania-Senegalese zone where  
112 the upwelling is seasonal (12°N-19°N), the zone off the Saharan bank (21°N-  
113 26°N), and the north Moroccan coast (26°N-35°N), the last two being characterized  
114 by year-round upwelling-favorable winds but with different intensities  
115 (Benazzouz et al., 2014).

116  
117 In this study, a recently developed bio-climatic modeling strategy has  
118 been applied. This model approach has been proven as an efficient tool for  
119 describing realistic responses of primary productivity and round sardinella  
120 to the environment (Auger et al., 2016, Brochier et al., 2018). A scheme  
121 of the modeling strategy applied in this study is shown in Fig. 2. Two  
122 different parts are identified. In a first step, a hindcast simulation from a  
123 coupled hydrodynamic/biogeochemical model produces a realistic 3-D simulation  
124 of variability in the fish environment in the CCUS over the period  
125 1980-2009. The hydrodynamic environment is simulated by the Regional  
126 Oceanic Modeling System ROMS (Shchepetkin and McWilliams, 2005) with  
127 an  $\sim 8$ -km resolution and 32 vertical sigma-levels for the CCUS, while the  
128 biogeochemical environment is simulated by the PISCES model (Pelagic Interaction  
129 Scheme for Carbon and Ecosystem Studies; see Aumont et al.,  
130 2003 and Aumont and Bopp, 2006) which simulates phytoplankton and zoo-  
131 plankton productivity based on the uptake of nutrients dispersed by ROMS  
132 currents. In the present work, the ROMS-PISCES coupled model was forced  
133 with the CFSR atmospheric reanalysis (Saha et al., 2010) at a 6-h timescale  
134 and with  $1/3^\circ$  resolution, and the lateral open boundary conditions are from

135 monthly model outputs from a simulation of the North Atlantic Ocean in  
136 which PISCES is forced by the NEMO hydrodynamic model (Nucleus for  
137 European Modelling of the Ocean; Madec, 2008). Please see Auger et al.  
138 (2015) for a description of the ROMS-PISCES model configuration, the forc-  
139 ing datasets, and the validation of model results using satellite data observa-  
140 tions. In a second step, the evolutionary individual-based model *Evol-DEB*  
141 (<https://github.com/tbrochier/EvolDEB>) was forced by physical and bio-  
142 geochemical outputs from ROMS-PISCES. *Evol-DEB* is an individual-based  
143 model that has been proven as an efficient tool to characterize the effect  
144 of climate on round sardinella population variables, accounting for environ-  
145 mental (e.g., currents, temperature and primary/secondary production) and  
146 biological (e.g., fish growth, mortality) factors. The performance of *Evol-*  
147 *DEB* has been assessed in the study area through a variety of comparisons  
148 including: 1) CPUE (Catch Per Unit Effort) indices calculated from local  
149 fisheries monitoring in Senegal and Mauritania, 2) observations of round  
150 sardinella body-length distribution from artisanal and industrial fisheries,  
151 scientific sampling, and oceanographic research vessels, 3) acoustic observa-  
152 tions from oceanographic research vessels, and finally 4) qualitative ecological  
153 knowledge from Senegalese fishermen. Brochier et al. (2018) provide a full  
154 description of *Evol-DEB* and the validation procedure. The three main envi-  
155 ronmental factors influencing the round sardinella dynamics that were tested  
156 in the *Evol-DEB* simulations and investigated in the current study were: 1)  
157 the currents, 2) the temperature, and 3) the food distribution (from a proxy  
158 based on the concentration of plankton in PISCES), each of them averaged  
159 over the ocean mixed layer. As described in Brochier et al. (2018), the tem-  
160 perature and food proxy were combined to define the *Habitat Quality Index*  
161 (*HQI*). In the *Evol-DEB* framework, each aggregation of round sardinella or  
162 *super-individuals* is affected by the *HQI* in such a way that the maximization  
163 of this *HQI* according to the environmental conditions determines the chance  
164 of survival of each super-individual. Round sardinella dynamics also depend  
165 on specific round sardinella parameters such as: 1) the swimming capacity, 2)  
166 the growth rate, 3) the functional response to the food, and 4) the preferred  
167 temperature. Please see Brochier et al. (2018) for details.

168  
169 In the present study, the *Evol-DEB* configuration that most realistically  
170 captures the response of round sardinella to the environment among all those  
171 tested in Brochier et al. (2018) was used: that in which adult populations  
172 are sensitive to the currents, and to the temperature and food distributions,

173 with maximum swimming speed of 4.5 body-length per second, and with  
174 the preferred temperature determined by the corresponding natal temper-  
175 ature. Each *Evol-DEB* simulation lasted for 30 years, from 1980 to 2009,  
176 with a seeding procedure taking place in 1980. The 1980-1984 period was  
177 viewed as a spin-up period, considering that the maximum longevity of super-  
178 individuals is  $\sim 4.5$  years. The choice of the initialization of environmental  
179 conditions was shown to have little effect on the subsequent emerging inter-  
180 annual variability, resulting therefore in an effective output period of 25 years  
181 (from 1985 to 2009). Please note that although the environmental forcings  
182 which influence round sardinella variability in *Evol-DEB* are the ocean vari-  
183 ables provided by *ROMS-PISCES*, the atmospheric forcing from the CFSR  
184 reanalysis used to run the *ROMS-PISCES* model do contain information of  
185 any potential teleconnection between the global climate and the local round  
186 sardinella population biomass. Therefore, the described comprehensive mod-  
187 eling framework (*ROMS-PISCES* and *Evol-DEB*) will capture a significant  
188 response to global climate forcing, depending on the forcing persistence and  
189 the noise generated internally by the models. If any climate-round sardinella  
190 teleconnection is identified in the analysis of final model outputs (Fig. 2),  
191 it must have entered into the model setup through the applied boundary  
192 conditions, and it should be strong enough to be passed among the physical-  
193 biogeochemical-ecosystem components of the models involved.

194

## 195 *2.2. Exploring the relation with the global climate*

196 The aim of this study was to understand how the latitudinal distribu-  
197 tion of simulated adult round sardinella biomass over the northwest African  
198 continental shelf is altered by changes in the local environmental conditions  
199 and to explore the possible role played by remote climate forcings. The  
200 biomass over the continental shelf captures most of the north-south round  
201 sardinella variability, as the stocks are generally tied to the coastal areas  
202 where the highest food production occurs. This feature is well represented  
203 by the *ROMS-PISCES-Evol-DEB* model framework (Figs. 3a-b). Based  
204 on the latter, various latitude vs months Hovmöller diagrams were plotted  
205 for different fields by averaging the corresponding variable across longitudes  
206 (Figs. 3c-f). To reduce the degrees of freedom and to efficiently characterize  
207 round sardinella variability, Empirical Orthogonal Function (EOF; Lorenz,  
208 1956) analysis was performed on the yearly Hovmöllers of modeled round sar-  
209 dinella biomass (anomalous round sardinella biomass averaged in longitude

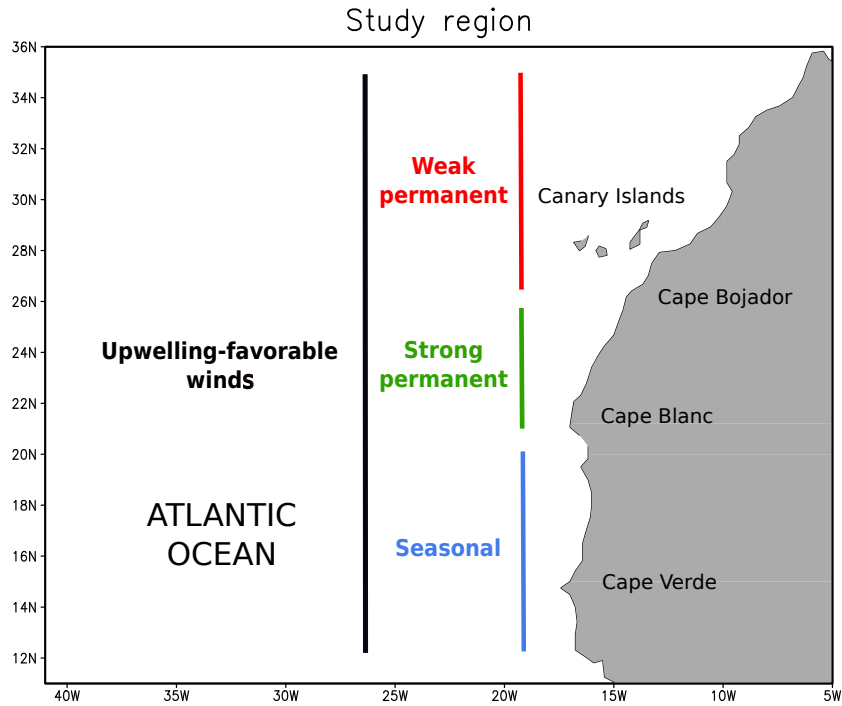


Figure 1: Study region and upwelling zones inside it. This figure is only used for illustrative purposes.

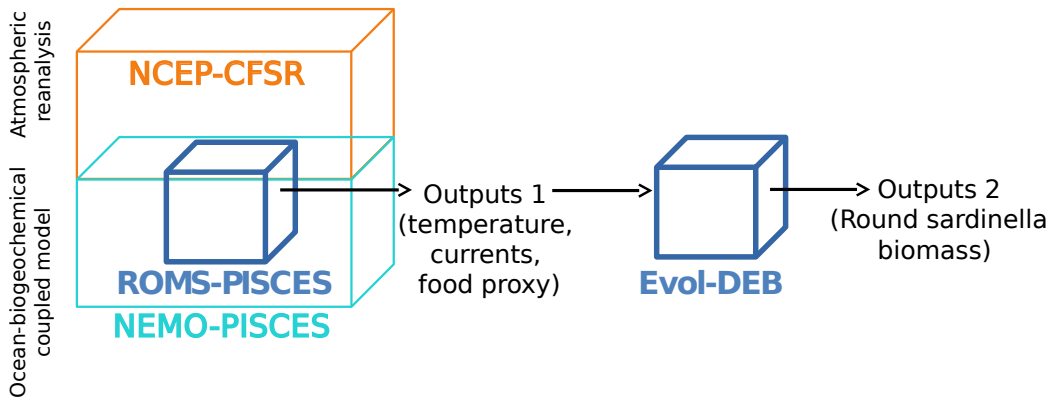


Figure 2: Modeling framework. The abbreviations used are: National Centers for Environmental Prediction (NCEP), Climate Forecast System Reanalysis (CFSR), Regional Oceanic Modeling System (ROMS), Pelagic Interaction Scheme for Carbon and Ecosystem Studies (PISCES), Nucleus for European Modelling of the Ocean (NEMO), and evolutionary individual-based model with dynamic energy budget (Evol-DEB)

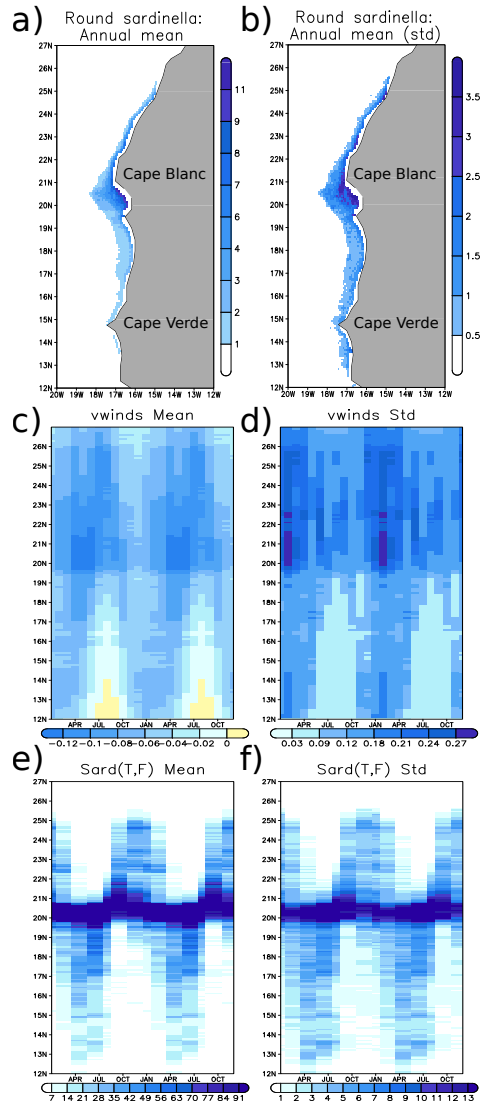


Figure 3: **Annual mean and seasonal cycles from the modeling framework.** In top panels the annual mean of round sardinella biomass (panel a), and the interannual variability of round sardinella biomass (in terms of standard deviation; panel b), from *Evol-DEB*. Units in tons/m<sup>2</sup>. Central panels: Seasonal cycles (mean in panel c, negative southward, and variability, in terms of standard deviation, in panel d) of the meridional component of the wind stress (from *ROMS-PISCES*; units in N/m<sup>2</sup>). Bottom panels: as panels c and d but for the simulated round sardinella biomass (from *Evol-DEB*; units in tons/m<sup>2</sup>). In the case of the meridional wind stress, the fields are averaged from the coast to the isobath 1000 meters.

210 along the northwest African coast). The associated standardized principal  
 211 components (PC) show the time evolution of the scores of the EOFs, thus  
 212 identifying the years in which these EOFs are manifest. The link between  
 213 these EOFs (or round sardinella modes) and the climate was evaluated in  
 214 terms of regression and composites maps. To analyze the link with the large-  
 215 scale environment (i.e., global climate), SST data from HadISST1 (Rayner  
 216 et al., 2003), and global observed sea level pressure data (SLP) and surface  
 217 winds from the NCEP Climate Forecast System Reanalysis (CFSR; Saha  
 218 et al., 2010) were used. The HadISST dataset was also used to calculate  
 219 the Niño 3.4 index (SST averages over the area 170-120°W, 5°S-5°N), and  
 220 the CFSR reanalysis was chosen to be consistent with the atmospheric condi-  
 221 tions prescribed in the *ROMS-PISCES* simulation. Sea temperature and  
 222 ocean currents averaged over the top 50 m of the water column (from *ROMS-*  
 223 *PISCES*) were used to characterize the local environmental variability (i.e.,  
 224 local climate). Please see the Table 1 for a summary of the data used in  
 225 the present study. The statistical significance was assessed by a bootstrap  
 226 re-sampling procedure with replacement. At the end of the study, a lead-lag  
 227 correlation analysis has been applied for exploring the predictive potential  
 228 of round sardinella distribution in the CCUS from equatorial Pacific SSTs.  
 229 In that case, the non-parametric test described by Ebisuzaki (1997), and  
 230 specially designed to avoid serial correlation, was used.

Table 1: Summary of the data used in the present study.

Variable	Source	Reference
(Global) SST	HadISST	Rayner et al. (2003)
(Global) SLP	CFSR	Saha et al. (2010)
(Global) Surface winds	CFSR	Saha et al. (2010)
Sea temperature	<i>ROMS-PISCES</i>	Auger et al. (2015)
Ocean currents	<i>ROMS-PISCES</i>	Auger et al. (2015)
Wind stress	<i>ROMS-PISCES</i>	Auger et al. (2015)
Round sardinella biomass	<i>Evol-DEB</i>	Brochier et al. (2018)

231 A linear regression prediction model was also constructed in the present  
 232 study to illustrate the potential of the results obtained for skillful prediction.  
 233 This prediction model is based on the “leave one out” method (Wilks, 2011),

234 which produces a forecast for each time  $t$  (year) using only data at other  
235 times (years) distinct from  $t$ .

### 236 **3. Results**

#### 237 *3.1. Anomalous migration further north of Cape Blanc*

238 The present modeling framework produces a coherent migration pattern  
239 of round sardinella population (Fig. 3e): to the south in spring reaching  
240 the Senegalese-Mauritanian waters in summer, and to the north in autumn,  
241 reaching the Saharan waters in winter (Corten et al., 2012). This migra-  
242 tion pattern from *Evol-DEB* is associated with the atmospheric conditions  
243 imposed on *ROMS-PISCES*. Evidence from that fact is the consistency be-  
244 tween the meridional wind stress ( $V_{st}$ , negative southward; see Fig. 3c) and  
245 the round sardinella biomass further north of Cape Blanc ( $\sim 21^\circ\text{N}$ ), a region  
246 characterized by strong alongshore currents to the south, in the so-called  
247 *Cape Blanc Transition Zone*. Only in early winter, when the southward  
248 wind stress in this area weakens (Fig. 3c), a certain percentage of round  
249 sardinella (those with the strongest swimming capacity) reach the Saharan  
250 waters (Fig. 3e), where the high food availability contributes to relatively  
251 high HQI all year round (Brochier et al., 2018). Interestingly, this minimum  
252 of southward wind stress in winter coincides with the strongest variability  
253 of this variable off Cape Blanc (Fig. 3d) and, with increased variance in  
254 round sardinella biomass north of that cape (Fig. 3f). The variability is  
255 expressed here in terms of the standard deviation, representing the degree  
256 of deviation of each variable with respect to its corresponding seasonal cycles.

257  
258 Hence, Fig. 3 points to the existence of year-to-year variability fur-  
259 ther north of Cape Blanc in both the environment and the round sardinella  
260 biomass. To assess the correlation between these variabilities, an EOF anal-  
261 ysis was performed on the yearly Hovmöllers of round sardinella biomass  
262 anomaly along the coast, from  $19^\circ\text{N}$  to  $26^\circ\text{N}$ , and for the January to March  
263 season. This season was selected in order to cover those months with the  
264 maximum variability in the alongshore wind stress ( $V_{st}$ ; Fig. 3d). The Prin-  
265 cipal Component (hereinafter PC1) of the leading EOF mode, which explain  
266 46% of the total variance, was then lag-regressed on the yearly Hovmöllers  
267 of round sardinella biomass (plotted from the previous July to the follow-  
268 ing June for a better comparison with the seasonal cycles; see Fig. 4a). A

269 dipole structure, with negative anomalies off the Saharan coast and posi-  
 270 tive anomalies off Cape Blanc was obtained from early to late winter. This  
 271 analysis indicates that anomalous meridional migration of round sardinella  
 272 may play a key role in determining the biomass and distribution of round  
 273 sardinella along the northwest African coast.

274

### 275 3.2. Role played by the environment

276 Firstly, the role of the environment in stimulating this leading mode of  
 277 variability was investigated by analyzing an additional *Evol-DEB* simulation  
 278 with climatological forcings obtained by averaging the ROMS-PISCES out-  
 279 puts for the entire period (1980-2009). That is, instead of forcing *Evol-DEB*  
 280 with the varying environmental conditions from 1980 to 2009 (*Inter experi-*  
 281 *ment* in Table 2), it was forced with the climatological averaged conditions  
 282 in that period (*Control experiment* in Table 2). Therefore the interannual  
 283 variability within the ROMS-PISCES outputs was removed such that this  
 284 simulation may be interpreted as a control simulation for *Evol-DEB*. EOF  
 285 analysis shows that the dipolar structure is missing in this control simulation  
 286 (Fig. 4b), indicating that the response in the *Inter experiment* was forced  
 287 by the environment.

Table 2: Overview of the set of *Evol-DEB* simulations run for the present study. Round sardinella dependence refers to those environmental parameters (Temperature, Food or both), from ROMS-PISCES, influencing the habitat quality of the species in *Evol-DEB*. Food contribution is quantified through a proxy defined as the sum of the biomass in the four PISCES plankton compartments (please see Brochier et al. 2018 for details).

Experiment	ROMS-PISCES forcing	round sardinella dependence
Inter	1980 – 2009	T,F
Control	$(1980 - 2009)_{avg}$	T,F
Inter T	1980 – 2009	T
Inter F	1980 – 2009	F

288

### 289 3.3. El Niño emerges as a potential forcing

290 Considering the important role of SSTs in the global climate teleconnec-  
 291 tions, next the PC1 from the *Inter experiment* was regressed on the global

Table 3: Linear correlations among the distinct PC1 obtained in the set of simulations recapitulated in Table 2.

Correlation	PC1(Control)	PC1(Inter T)	PC1(Inter F)
PC1(Inter)	0.02	0.88	0.41

292 SSTs of the same season. A noticeably clear and significant ENSO pattern  
 293 emerged in the tropical Pacific (Fig. 5a). The same ENSO structure ap-  
 294 peared when just an index based on the averaged accumulation of round  
 295 sardinella off Cape Blanc was projected onto the SSTs (not shown). The  
 296 question emerging therefore is whether this anomalous response of round sar-  
 297 dinella in northwest Africa (the aforementioned dipolar structure) is caused  
 298 by ENSO or if it is a statistical artifact.

299

300 Before exploring the dynamical mechanisms linking ENSO and round sar-  
 301 dinella spatio-temporal variability, the environmental response to ENSO in  
 302 northwest Africa that causes the anomalous distribution of modeled round  
 303 sardinella biomass along the coast was investigated. To address this ques-  
 304 tion, recall that both temperature and food distribution influence the HQI  
 305 in the previously described *Evol-DEB* simulations (*Inter Experiment & Con-*  
 306 *trol Experiment*), as these follow the more realistic configuration according  
 307 to Brochier et al. (2018). Assuming that the sardinella dependence on their  
 308 habitat quality is based only on the food availability (*Inter F experiment* in  
 309 Table 2) leads to the disappearance of the previously analyzed dipolar struc-  
 310 ture (Fig. 6c). However, this is not the case when the HQI is based only on  
 311 sea temperature (Fig. 6a). Therefore it could be concluded that the dipolar  
 312 structure identified in Fig. 4a is associated with the round sardinella’s depen-  
 313 dence on water temperature as represented in the model. Please note that  
 314 this does not mean that round sardinella only follows the variability of the  
 315 water temperature. Others factors, such as alongshore currents, could also  
 316 play a major role in altering the round sardinella variability. However, this  
 317 major role would only emerge when round sardinella migrates towards areas  
 318 with optimal temperature conditions. If this dependence on the temperature  
 319 is removed, the effect of ENSO on round sardinella also disappears. This  
 320 effect of temperature on the teleconnection is reinforced by the correlations  
 321 among the leading principal components of round sardinella’s biomass in the

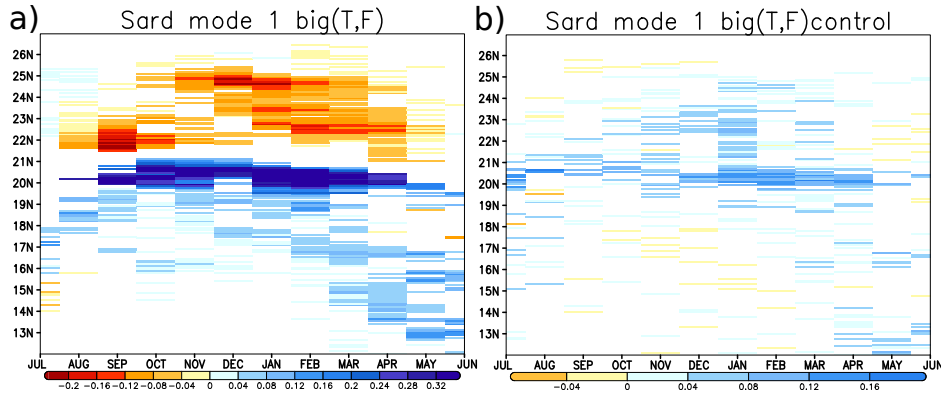


Figure 4: **Round sardinella EOF: a mode forced by the environment.** Leading EOF of the anomalous sardinella biomass (calculated from 19°N to 26°N and for the JFM season; units in tons/m<sup>2</sup> per std in the PC1) obtained in: a) the Inter experiment and b) the Control experiment. Shading areas represent the 90% significant response according to a bootstrap technique with replacement. Please note that blue and red colors indicate positive and negative anomalies of biomass respectively.

322 different simulations (see Table 3). Furthermore, the regression maps of the  
 323 leading PCs on global SSTs showed that the ENSO pattern persists when  
 324 the round sardinella dependence on food is removed (Inter T experiment; see  
 325 Fig. 6b), but disappears when the round sardinella dependence on tempera-  
 326 ture is removed (Inter F experiment; see Fig. 6d).

327  
 328 There is still a remaining aspect to fully characterize the ENSO-round  
 329 sardinella teleconnection: its linearity in relation to the ENSO phase. In  
 330 particular, the question emerging is whether the identified ENSO signal is  
 331 caused by the influence of both warm (El Niño) and cold (La Niña) ENSO  
 332 phases. Comparing the evolution of the Niño 3.4 index and the standardized  
 333 round sardinella PC1 (Inter Experiment) revealed that the three highest val-  
 334 ues of PC1 coincide with three (1988, 1998, 2003) of the four highest values  
 335 of the Niño 3.4 index. Nevertheless, there is an absence of coincidence in  
 336 time between the negative values of the Niño 3.4 index and the peaks of  
 337 the round sardinella PC1. This appears more clearly when comparing the  
 338 negative composite patterns (those years in which the index is below -1 stan-  
 339 dard deviation) of SSTs for the Niño 3.4 index and the round sardinella PC1  
 340 (Supplementary material; Fig. S1): this indicates that a negative occurrence  
 341 of the round sardinella mode is more related to the NAO than to the Pacific

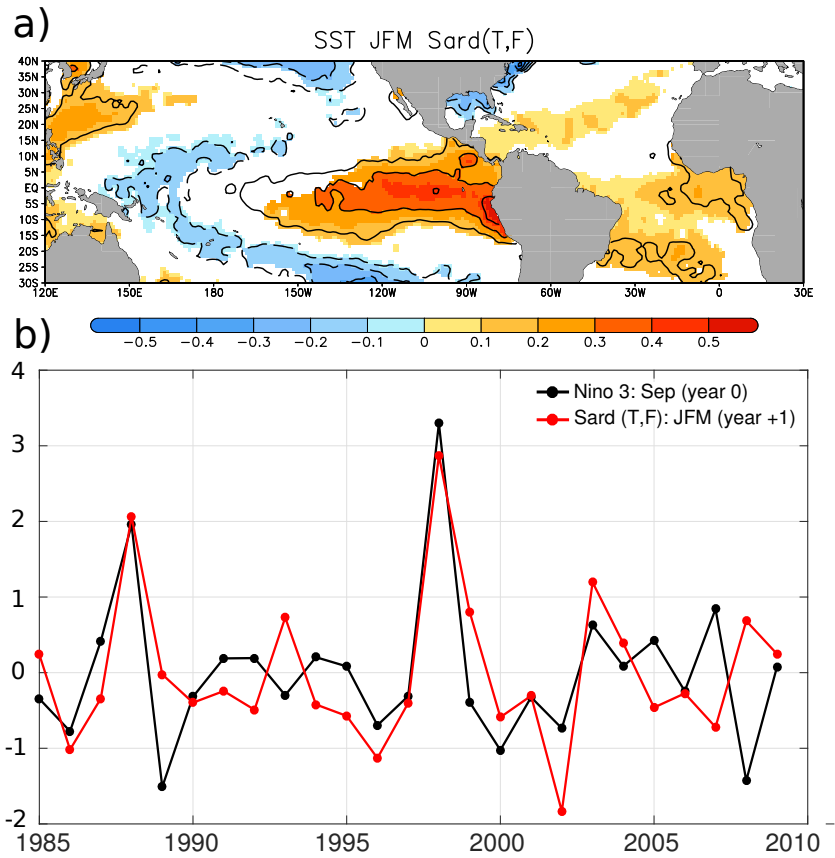


Figure 5: **Round sardinella EOF: a mode forced ENSO.** a) Regression map of the round sardinella mode of biomass on anomalous SSTs (units in degrees per std in the PC1); shading areas represent the 90% significant response according to a bootstrap technique with replacement. b) standardized PC1 of the round sardinella mode (red line) and the standardized Niño 3.4 index in the previous September (black line).

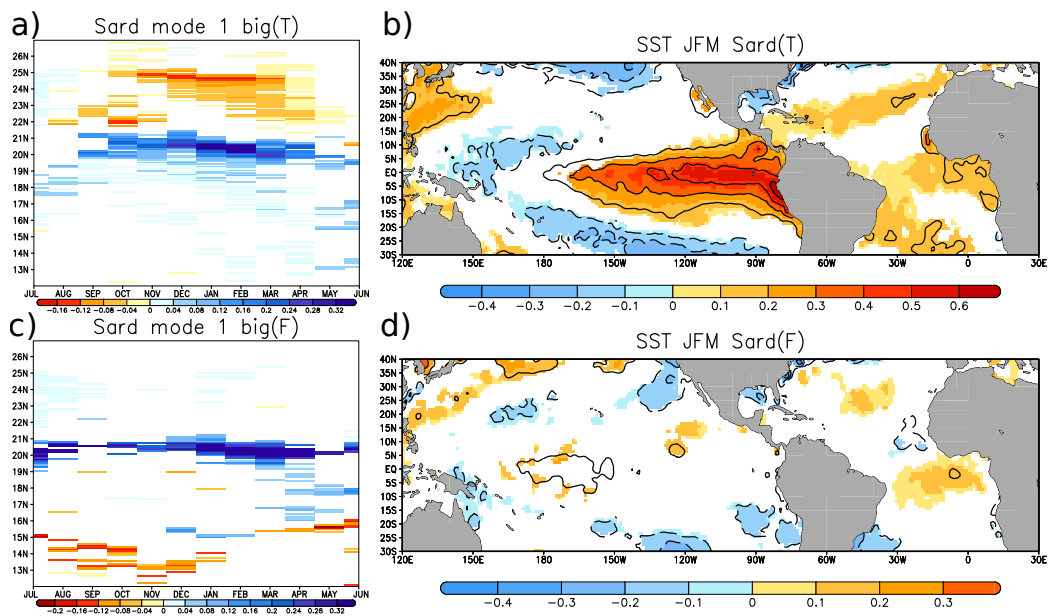


Figure 6: **Round sardinella EOF: a mode highlighting the role of temperature.** a) leading EOF of anomalous sardinella biomass for the Inter T Experiment, b) SST regression for the Inter T Experiment, c) leading EOF of anomalous sardinella biomass for the Inter F Experiment, d) SST regression for the Inter F Experiment. Shading areas represent the 90% significant response according to a bootstrap technique with replacement.

342 SSTs. Thus, the ENSO-round sardinella link found in the described model-  
343 ing framework is only triggered by warm ENSO phases (El Niño).

344

### 345 *3.4. Dynamical mechanisms*

346 To address the dynamical explanations supporting this influence of El  
347 Niño episodes on the modeled round sardinella biomass, early winter (from  
348 November to January) and late winter (from February to March) were sepa-  
349 rated based on: 1) the different evolution of El Niño episodes and their related  
350 responses in the TNA, and 2) the very different feature of round sardinella  
351 migrations along the northwest African coast before and after January. Re-  
352 garding the former, the response to ENSO in early winter is characterized by  
353 anomalous horizontal and vertical flows in the western TNA (Wang, 2002)  
354 and by an East Atlantic (EA) like pattern further north over the North At-  
355 lantic (King et al., 2018). From January onwards, an atmospheric Rossby  
356 wavetrain forced from the tropical Pacific crosses the North Pacific-American  
357 region and reaches the TNA (Enfield and Mayer, 1997). This response, to-  
358 gether with the documented ENSO influence on the Walker and Atlantic  
359 Hadley circulation cells (Wang, 2004), explains the ENSO-TNA teleconnec-  
360 tion in late winter. Regarding the round sardinella migrations along the  
361 northwest African coast, remarkable differences are also identified between  
362 early and late winter. Before January, round sardinella are normally moving  
363 northward to reach the Saharan waters (see Fig. 3e), where there is high food  
364 availability resulting in high HQI (Brochier et al., 2018). After January, how-  
365 ever, round sardinella begin a southward migration. The underlying reasons  
366 include the declining food production when upwelling off Cap Blanc retracts  
367 to very coastal waters, and the drop in water temperature to values below the  
368 species tolerance. Furthermore, it is worth reminding that a natural instinct  
369 of round sardinella to search its natal homing temperature is implemented  
370 in Evol-DEB. Thus, as both the upwelling intensity and the water tempera-  
371 ture could be altered by the El Niño influence in the study region, a related  
372 response in round sardinella is expected.

373

#### 374 *3.4.1. Early-winter*

375 In early-winter (Fig. 7a), a marked El Niño pattern is identified in those  
376 years in which the anomalous round sardinella mode (Fig. 6a) is manifested.  
377 A weakening of the trade winds has been identified in the western TNA, in

378 agreement with the documented response to ENSO (Wang, 2002). The resul-  
379 tant anomalous northward winds turn right at approximately 25-30°N. This  
380 deflection is explained by the EA-like pattern found over the North Atlantic  
381 and is consistent with the most recent literature (King et al., 2018). Conse-  
382 quently, an anomalous increase of the subtropical winds is detected to the east  
383 that reaches the African continent. For illustrative purposes, the significant  
384 response of the surface wind (black vectors in Fig. 7a) is calculated with re-  
385 spect to the zonal component in Nov-Jan. In the ROMS-PISCES simulation,  
386 this global signal is associated with a significant increase of the zonal wind  
387 stress to the east (black vectors in Figs. 8a-b) and, even more important for  
388 this case, with an anomalous increase of the alongshore currents to the south  
389 (shaded areas in Fig. 8b). Note that this enhancement of the alongshore cur-  
390 rents is particularly intense off Cape Bojador and Cape Blanc, although it is  
391 not associated with significant upwelling-favorable wind anomalies. Off Cape  
392 Blanc, it appears to coincide with the anomalous accumulation of round sar-  
393 dinella biomass simulated by *Evol-DEB* (Fig. 6a). Thus, the response to El  
394 Niño drives anomalous southward alongshore currents in early winter, along  
395 the *Cape Blanc Frontal Zone*, that counters the normal northward migration  
396 of round sardinella. As a consequence, an anomalous increase (decrease) of  
397 biomass emerges at  $\sim 20\text{-}21^\circ\text{N}$  ( $\sim 24\text{-}25^\circ\text{N}$ ).

398

### 399 3.4.2. *Later-winter*

400 In late winter, the round sardinella mode is related to northward wind  
401 anomalies in the eastern part of the TNA that occur after the peak of El Niño  
402 episodes and which are particularly intense along the northwest African coast  
403 (the significant signal of the meridional component is highlighted as black  
404 vectors in Fig. 7b). The weakened Azores high identified in Fig. 7b is in  
405 agreement with the documented late winter influence of ENSO caused by the  
406 thermally-driven direct circulation (Wang, 2004) and Rossby wave activity  
407 (Enfield and Mayer, 1997). The anomalous SST pattern identified here is also  
408 as expected (Ham et al., 2014). The resultant alongshore winds in northwest  
409 Africa weakens the upwelling due to a reduction of the Ekman transport and  
410 hence, an intense and significant anomalous warming is detected along the  
411 coast. The ROMS-PISCES model reproduces the anomalous warming along  
412 the coast as a consequence of the attenuated coastal upwelling (Fig. 8c) and  
413 simulates northward coastal current anomalies (Fig. 8d).

414

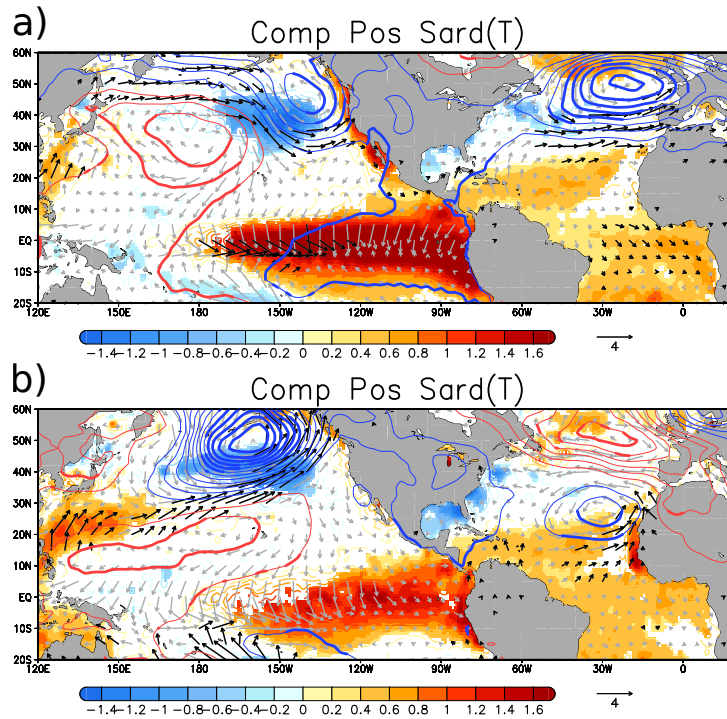


Figure 7: **Global signature of the round sardinella mode.** a) positive composite maps in early winter based on the standardized PC1 of the anomalous sardinella mode (years above 1 standard deviation), b) as in a) but for late winter. In both cases the fields plotted are: anomalous SST (shaded the significant response; units in degrees), anomalous SLP (contoured; thick contoured the significant response), and anomalous surface wind (grey vectors; units in m/s). Significance at the 90% level based on a bootstrap technique with replacement.

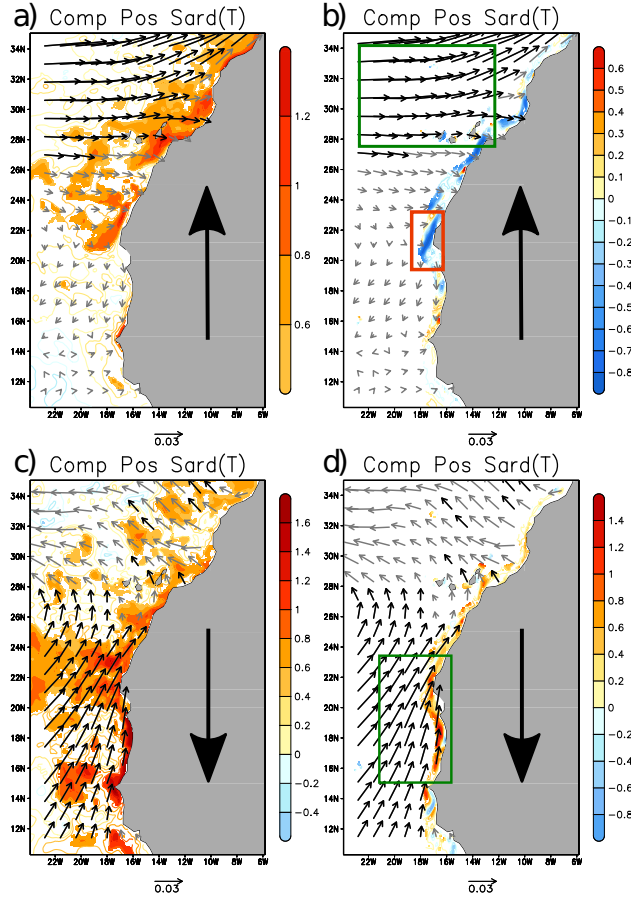


Figure 8: **Local signature of the round sardinella mode (ROMS-PISCES).** Upper panels correspond to the composites maps in early winter (Nov-Jan) and bottom panels to the composites maps in late winter (Feb-Mar). Left panels show the anomalous temperature in the top 50 meters of the water column (shaded the significant response; units in degrees). In the right panels the anomalous meridional currents of the top 50 meters of the water column (shaded the significant response, units in  $10 \times \text{m/s}$ ). The anomalous wind stress (vectors; units in  $\text{N/m}^2$ ) are shown on all panels. Only the water surfaces with less than 1000 meters depth are plotted due to these waters house the vast majority of round sardinella. The significant response in the zonal (meridional) anomalous wind stress is highlighted for early (late) winter with black vectors. Significance at the 90% level based on a bootstrap technique with replacement. Large pointing-arrows indicate the migration pattern of the species in early and late winter according to the seasonal cycle of biomass.

415 To understand the round sardinella response, it is important to realize  
416 that although the presence of the species has been reported in a very large  
417 range of temperatures, from  $\sim 10^{\circ}\text{C}$  in the Mediterranean Sea (Tsikliras and  
418 Antonopoulou, 2006) up to  $29^{\circ}\text{C}$  in Senegal (Marchal, 1991), the highest  
419 biomass in northwest Africa has been detected for a range of SSTs between  
420  $21^{\circ}\text{C}$  and  $25^{\circ}\text{C}$  (Diankha et al., 2015). Thus, waters excessively cold (be-  
421 low  $19^{\circ}\text{C}$ ) or excessively warm (above  $26\text{-}27^{\circ}\text{C}$ ) host low round sardinella  
422 biomass. This feature is included in Evol-DEB by a correction factor applied  
423 to all the energy fluxes between the model compartments. Thus, one can  
424 understand why in late winter, under normal conditions, the drop of water  
425 temperatures off the Saharan bank to values below  $19^{\circ}\text{C}$  contributes to a  
426 southward migration (favored by the climatological southward currents) of  
427 round sardinella.

428  
429 In this context, the anomalous warming generated by El Niño in late  
430 winter off the African coast (Fig. 8c) increases the absolute temperature of  
431 the water column off Cape Blanc to around  $20^{\circ}\text{C}$ , significantly warmer than  
432 the normal  $\sim 18^{\circ}\text{C}$  there at that time of the year (see also Fig. S2 in Supple-  
433 mentary material). This fact, together with the reduced passive advection  
434 of round sardinella due to the anomalous weakening of the southward cur-  
435 rents south of Cape Blanc during El Niño years (Fig. 8d), explains how the  
436 anomalous accumulation of biomass at  $20\text{-}21^{\circ}\text{N}$  latitude identified in Evol-  
437 Deb in association with the leading EOF mode (Fig. 6a) persists until well  
438 into the spring season. However, the persistence of negative biomass anoma-  
439 lies further north of Cape Blanc seems to be a reminiscent effect of the fewer  
440 individuals who reached the Saharan waters at the beginning of the winter  
441 season. The slight positive biomass anomalies detected between  $13^{\circ}\text{N}$  and  
442  $19^{\circ}\text{N}$  (Fig. 4a) in late winter might reflect the response of round sardinella  
443 to the warmer and more favorable water temperature conditions along the  
444 Mauritanian-Senegalese coast as a consequence of the reduced upwelling.

### 445 446 *3.5. Potential predictability of round sardinella population biomass*

447 One of the main contributions of this work is that it provides the basis for  
448 the development of a future seasonal forecasting tool of round sardinella lat-  
449 itudinal distribution along northwest Africa based on El Niño-related SSTs,  
450 which can be observed from the space. In particular, high lagged correlations  
451 between the round sardinella mode in winter (see Fig. 6a) and the Niño 3

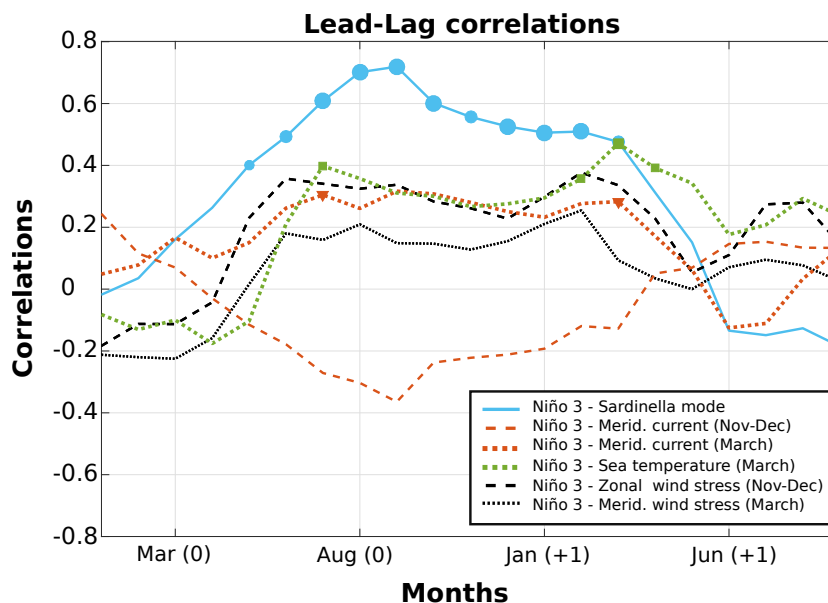


Figure 9: **Lead-lag correlations.** Blue solid line shows the linear correlation between the Niño 3 index at different lags and the leading sardinella mode (i.e., the corresponding PC) in JFM (year +1; see Fig. 6a). The same correlations with the Niño 3 index are shown for: 1) the meridional current (top 50m of the water column) off Cape Blanc in Nov-Dec (dashed brown line) and March (dotted brown line), and 2) the water temperature (top 50m of the water column) off Cape Blanc in March (green dotted line). The region off Cape Blanc is defined as the area within the red square indicated in Fig. 8b. Large, medium and small sized symbols represent correlations at the 99%, 95% and 90% confidence level respectively according to Ebisuzaki (1997). Black dashed (dotted) line shows the correlation between the leading round sardinella mode and the zonal (meridional) wind stress averaged within the green boxes of Fig. 8.

452 index suggest the potential for skillful prediction (see blue line in Fig. 9).  
 453 The El Niño-round sardinella link appears stronger with the eastern tropical  
 454 Pacific than with the central tropical Pacific (Supplementary material; Fig.  
 455 S3), which is consistent with the available literature related to the ENSO-  
 456 TNA teleconnection (Taschetto et al., 2016).

457

458 A linear regression prediction model based on the “leave one out” method  
 459 (Wilks, 2011) has been constructed to predict, for the two strongest Eastern  
 460 El Niño episodes of the simulated period (1987/88 and 1997/98), the anoma-  
 461 lous distribution of round sardinella from El Niño 3 SSTs in the previous  
 462 September. The resultant predictions and the corresponding patterns esti-

463 mated by *Evol-DEB* are shown in Figure 10. One could reasonably think that  
464 our prediction skill, based on the leading EOF of round sardinella biomass in  
465 winter, should be almost completely dependent on the information coming  
466 from the specific episodes to be predicted, as they correspond to extreme val-  
467 ues of the aforementioned EOF. However, if so, the forecast skill assessed with  
468 our cross-validation method should be close to zero. As shown in Fig. 10a-d,  
469 this is not the case: the anomalous SSTs in the Niño 3 region in Septem-  
470 ber (i.e., September 1987 and September 1997, respectively) are enough to  
471 predict realistically the anomalous distribution of round sardinella in the  
472 following winter and spring along the northwest African coast. Although  
473 robust, this predictive skill seems to be only valid for eastern (and partic-  
474 ularly strong) El Niño years, as appreciated in the comparison between the  
475 modeled and the predicted evolution of round sardinella population biomass  
476 in a particular location (Cape Blanc; see bottom panel in Fig. 10e).

477

#### 478 4. Summary and discussions

479 The present study provides, for the first time, a consistent mechanism  
480 explaining how a remote climatic phenomenon (El Niño, understood as the  
481 ENSO warm phases) is able to alter the latitudinal migration pattern of  
482 *Sardinella aurita* (or round sardinella) in the narrow coastal band along  
483 northwest Africa. This has been possible through an innovative modeling  
484 strategy specifically designed to explore potential environmental drivers of  
485 spatio-temporal population variability of this species in the region. This  
486 modeling framework has been previously validated in the study region and  
487 highlighted the strong effect that the local environment may play on the dis-  
488 tribution of round sardinella along this coast (Brochier et al., 2018).

489

490 Modeling results point out that the round sardinella response to El Niño  
491 is an anomalous migration pattern of this species during boreal winter be-  
492 tween the Mauritanian and the Saharan waters. As a consequence, the model  
493 simulates an anomalous increase (decrease) of round sardinella biomass off  
494 the Cape Blanc (Saharan coast) during El Niño years. Distinct bio-physical  
495 mechanisms take place in early and late winter to sustain this modeled ma-  
496 rine ecological response to El Niño (if needed, see scheme in Fig. S4 of  
497 Supplementary material). This difference between early and late winter is  
498 not really surprising, as 1) the climatological responses to El Niño evolve

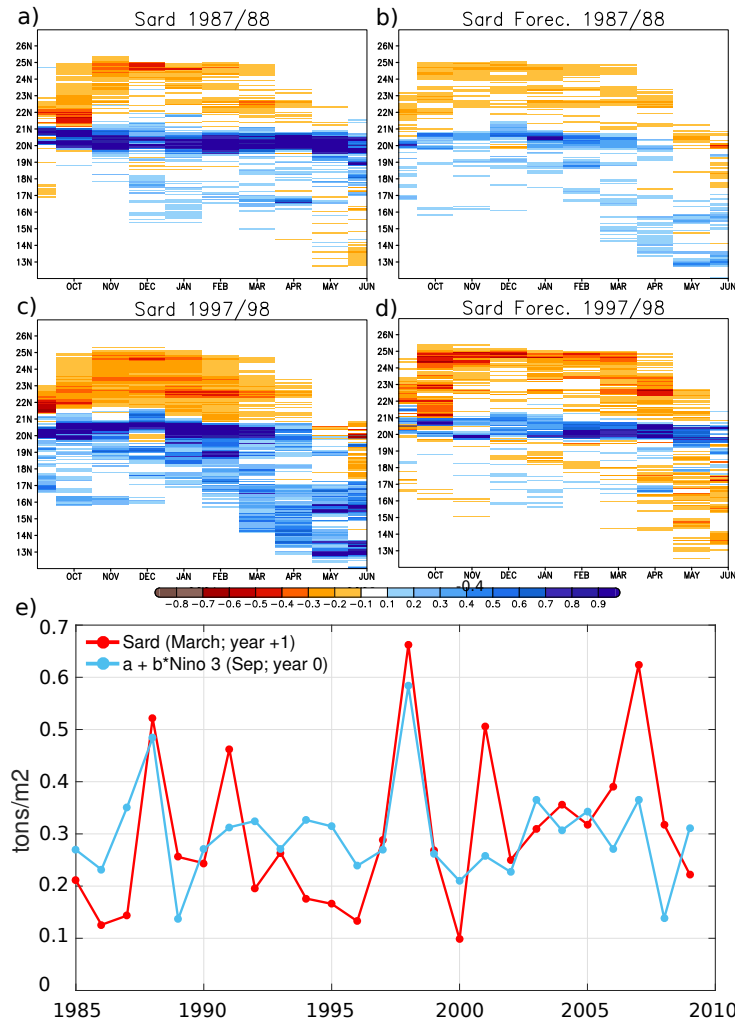


Figure 10: **Potential predictability.** Round sardinella biomass anomaly from *Evol-DEB* in: a) 1987/1988 and c) 1997/1998. Prediction of the modeled round sardinella biomass anomaly (from El Niño 3 SSTs in the previous September) in: b) 1987/1988 and d) 1997/1998. Units in tons/m<sup>2</sup>. In the bottom panel the time evolution of the round sardinella biomass in March off Cape Blanc from *Evol-DEB* (red line) and its prediction from El Niño 3 SSTs in the previous September (blue line).

499 over time along the winter months and 2) the dynamical feature of round  
500 sardinella off northwest Africa is completely different before and after Jan-  
501 uary, being characterized by a northward migration (searching the Saharan  
502 bank) in the former case, but by a southward migration, avoiding the cold  
503 conditions in the Saharan waters from January onwards, in the latter case.  
504 Accordingly, the specific responses to El Niño identified in the described  
505 modeling framework and the proposed mechanisms in each sub-season are:

- 506 • In early winter (November-January), a weakened northward migration  
507 of round sardinella. This signal could be explained by an anomalous  
508 enhancement of the alongshore currents to the south, off the Cape  
509 Blanc region, due to the El Niño influence.
- 510 • In late winter (February-March), an anomalous accumulation of round  
511 sardinella off Cape Blanc, the underlying mechanism being twofold: 1)  
512 through a weakening of the alongshore currents to the south (reducing  
513 the passive advection component of the southward migrations of round  
514 sardinella) and 2) through an anomalous warming of the surface ocean  
515 due to a reduction of the coastal upwelling (which improve the habitat  
516 conditions of round sardinella).

517 Summarizing, the El Niño-round sardinella teleconnection simulated here  
518 is mainly explained by the modulating role that the anomalous alongshore  
519 currents forced by El Niño in the *Cape Blanc Frontal Zone* exerts on the nor-  
520 mal migration of this species when it avoids water temperatures out of the  
521 species tolerance and when it follows temperatures close to its natal homing  
522 conditions. Thus, a general conclusion from the results of this study is that  
523 a realistic response to El Niño in both, sea temperature and coastal currents,  
524 is crucial to produce the teleconnection proposed. From a large-scale per-  
525 spective, there is an extensive literature explaining the dynamical aspects  
526 associated with the ENSO-TNA teleconnection and it is not a major goal of  
527 this work to explain this in depth. However, it is worth mentioning how the  
528 mechanisms presented here are consistent with those accepted by the climate  
529 community (Enfield and Mayer, 1997, Wang, 2002, 2004, Ham et al., 2014,  
530 King et al., 2018), reinforcing therefore the robustness of the El Niño-round  
531 sardinella teleconnection.

532  
533 Although a full validation of the El Niño-round sardinella teleconnection  
534 is an extremely challenging issue due to the scarcity of reliable data on the

535 time varying distribution and abundance fish population, the modeling ap-  
536 proach presented here seems to be able to simulate a robust ENSO response of  
537 the environmental conditions off Cape Blanc in winter, closely related to the  
538 ENSO induced effects in round sardinella biomass (Supplementary material;  
539 Fig. S5). In this respect, it is worth mentioning that the water tempera-  
540 ture and ocean current responses described here are consistent with those  
541 identified in February-March 1998 after the peak of one of the strongest El  
542 Niño episodes of the last decades (Zeeberg et al., 2008). This reinforces the  
543 theory of an influence of El Niño on the hydrodynamic conditions along the  
544 Mauritanian-Saharan coast. This fact, together with the validated skill of  
545 the modeling strategy used to simulate realistic responses of round sardinella  
546 to the local environment (Brochier et al., 2018), substantiates the findings of  
547 this work.

548  
549 In contrast to the major role that food availability plays for determining  
550 sardine and anchovy abundance in the northern part of the CCUS (Sánchez-  
551 Garrido et al., 2019), the present analyses indicate that the alteration of the  
552 variability in nutrient abundance associated with El Niño seems to play a  
553 minor role for the El Niño-round sardinella teleconnection. This is actually  
554 consistent with previous works which suggest that the currents and the wa-  
555 ter temperature are the main environmental variables influencing the round  
556 sardinella variability in the southern part of this upwelling system (Zeeberg  
557 et al., 2008, Bacha et al., 2017). However, other studies argue for a weaker  
558 (Roy and Reason, 2001, Arístegui et al., 2006) or an absent (Cropper et al.,  
559 2014, Oettli et al., 2016, Gómez-Letona et al., 2017) link between ENSO and  
560 the northwest African environmental conditions. This apparent inconsistency  
561 can be explained by diverse causes, such as 1) the distinct manifestations of  
562 the CCUS variability to the methodology applied (Benazzouz et al., 2014)  
563 or 2) the fact that in this study, the degrees of freedom of the entire spatio-  
564 temporal variability of round sardinella were reduced by using the latitude  
565 as a measure of spatial location (by averaging the biomass in longitude over  
566 the continental shelf) and by focusing the analysis on a particular mode of  
567 variability. All this could have contributed to a more efficient identification  
568 of the El Niño related response in this study.

569  
570 Furthermore, it should not be ruled out that round sardinella could act  
571 as an ecological integrator of El Niño influence on northwest Africa, show-  
572 ing even higher correlations than those obtained through the use of other

573 environmental fields (e.g., water temperature, currents, or Chl-a), which  
574 intuitively should be more directly influenced by a remote climate forcing  
575 (Di Lorenzo and Ohman, 2013). Indeed, the round sardinella mode ana-  
576 lyzed here presents higher correlations with the Niño index than with the  
577 local environment (wind stress, meridional current and sea temperature) off  
578 northwest Africa (Fig. 9). This striking feature had been already found for  
579 other ecological impacts of ENSO (Capa-Morocho et al., 2014, Diouf et al.,  
580 2017). The present study suggests a capacity of round sardinella to integrate  
581 the non-linearities among the climate variables in a unique mode of biomass  
582 variability.

583

584 We are aware of the intrinsic limitations of the modeling approach used in  
585 this study, and we do not expect a perfect match between the real (ideally ob-  
586 served) and the simulated responses of round sardinella to the environment.  
587 Nevertheless, this approach provides a highly valuable measure of how the  
588 spatio-temporal variability of round sardinella reacts to actual climate forc-  
589 ings (Brochier et al., 2018). Thus, we believe that this study represents a  
590 valuable step forward in relation to how the global climate can alter local  
591 responses in marine ecosystems. Furthermore, given that enhanced global re-  
592 sponses to ENSO are expected under a warmer climate (Frauen et al., 2014),  
593 the El Niño-round sardinella teleconnection might enhance within the next  
594 decades. This and other related questions should be further analyzed in fu-  
595 ture works.

596

## 597 **Acknowledgments**

598 The authors thank Davide Zanchettin and Patrice Brehmer for their use-  
599 ful comments and support during the development of this study. This work  
600 was funded by the european PREFACE project (No. 603521, Enhancing pre-  
601 diction of tropical Atlantic climate and its impacts <http://preface.b.uib.no>)  
602 and by the european TRIATLAS project (No. 817578, South and tropical  
603 Atlantic climate-based marine ecosystem prediction for sustainable manage-  
604 ment). Additional support during the writing phase (for P.A. Auger) was  
605 provided by the Instituto Milenio de Oceanografía (IMO-Chile), funded by  
606 the Iniciativa Científica Milenio (ICM-Chile).

607 **References**

- 608 Arístegui, J., Alvarez-Salgado, X. A., Barton, E. D., Figueiras, F. G.,  
609 Hernandez-Leon, S., Roy, C., Santos, A., 2006. Oceanography and fish-  
610 eries of the canary current/iberian region of the eastern north atlantic  
611 (18a, e). The global coastal ocean: Interdisciplinary regional studies and  
612 syntheses 14, 879.
- 613 Auger, P.-A., Gorgues, T., Machu, E., Aumont, O., Brehmer, P., Nov. 2016.  
614 [DATASET] What drives the spatial variability of primary productivity  
615 and matter fluxes in the north-west African upwelling system? A modelling  
616 approach. Biogeosciences 13, 6419–6440.
- 617 Auger, P. A., Machu, E., Gorgues, T., Grima, N., Waeles, M., 2015. Compar-  
618 ative study of potential transfer of natural and anthropogenic cadmium to  
619 plankton communities in the north-west african upwelling. Science of the  
620 Total Environment 505, 870–888.
- 621 Aumont, O., Bopp, L., Jun. 2006. Globalizing results from ocean in situ iron  
622 fertilization studies. Global Biogeochemical Cycles 20, GB2017.
- 623 Aumont, O., Maier-Reimer, E., Blain, S., Monfray, P., Jun. 2003. An ecosys-  
624 tem model of the global ocean including Fe, Si, P colimitations. Global  
625 Biogeochemical Cycles 17, 29–1.
- 626 Bacha, M., Jeyid, M. A., Vantrepotte, V., Dessailly, D., Amara, R., 2017.  
627 Environmental effects on the spatio-temporal patterns of abundance and  
628 distribution of sardina pilchardus and sardinella off the mauritanian coast  
629 (north-west africa). Fisheries Oceanography 26 (3), 282–298.
- 630 Báez, J., Santamaría, M., García, A., Gonzalez, J., Hernández, E., Ferri-  
631 Yáñez, F., 2019. Influence of the arctic oscillations on the sardine off  
632 northwest africa during the period 1976-1996. VIE ET MILIEU-LIFE AND  
633 ENVIRONMENT 69 (1), 71–77.
- 634 Bakun, A., 1990. Global climate change and intensification of coastal ocean  
635 upwelling. Science 247 (4939), 198–201.
- 636 Bakun, A., Black, B. A., Bograd, S. J., Garcia-Reyes, M., Miller, A. J.,  
637 Rykaczewski, R. R., Sydeman, W. J., 2015. Anticipated effects of climate

- 638 change on coastal upwelling ecosystems. *Current Climate Change Reports*  
639 1 (2), 85–93.
- 640 Barton, E., Aristegui, J., Tett, P., Cantón, M., Garcia-Braun, J., Hernández-  
641 León, S., Nykjaer, L., Almeida, C., Almunia, J., Ballesteros, S., et al.,  
642 1998. The transition zone of the canary current upwelling region. *Progress in*  
643 *Oceanography* 41 (4), 455–504.
- 644 Benazzouz, A., Mordane, S., Orbi, A., Chagdali, M., Hilmi, K., Atillah,  
645 A., Pelegrí, J. L., Hervé, D., 2014. An improved coastal upwelling index  
646 from sea surface temperature using satellite-based approach—the case of the  
647 canary current upwelling system. *Continental Shelf Research* 81, 38–54.
- 648 Bez, N., Braham, C.-B., 2014. Indicator variables for a robust estimation of  
649 an acoustic index of abundance. *Canadian journal of fisheries and aquatic*  
650 *sciences* 71 (5), 709–718.
- 651 Binet, D., 1988. Rôle possible d’une intensification des alizés sur le change-  
652 ment de répartition des sardines et sardinelles le long de la côte ouest  
653 africaine. *Aquatic living resources* 1 (2), 115–132.
- 654 Boëly, T., Chabanne, J., Fréon, P., Stéquert, B., 1978. Cycle sexuel et migra-  
655 tions de sardinella aurita sur le plateau ouest-africain des îles bissagos à la  
656 mauritanie. In: *Symp. sur le courant des Canaries: upwelling et ressources*  
657 *vivantes*. Las Palmas. No. 92. pp. 1–12.
- 658 Braham, C.-B., Fréon, P., Laurec, A., Demarcq, H., Bez, N., 2014. New  
659 insights in the spatial dynamics of sardinella stocks off mauritania (north-  
660 west africa) based on logbook data analysis. *Fisheries Research* 154, 195–  
661 204.
- 662 Brochier, T., Auger, P.-A., Pecquerie, L., Machu, E., Capet, X., Thiaw, M.,  
663 Mbaye, B. C., Braham, C.-B., Ettahiri, O., Charouki, N., et al., 2018.  
664 [DATASET] Complex small pelagic fish population patterns arising from  
665 individual behavioral responses to their environment. *Progress in Oceanog-*  
666 *raphy* 164, 12–27.
- 667 Brochier, T., Echevin, V., Tam, J., Chaigneau, A., Goubanova, K., Bertrand,  
668 A., 2013. Climate change scenarios experiments predict a future reduction  
669 in small pelagic fish recruitment in the humboldt current system. *Global*  
670 *change biology* 19 (6), 1841–1853.

- 671 Capa-Morocho, M., Rodríguez-Fonseca, B., Ruiz-Ramos, M., 2014. Crop  
672 yield as a bioclimatic index of el niño impact in europe: Crop forecast  
673 implications. *Agricultural and forest meteorology* 198, 42–52.
- 674 Carr, M.-E., Kearns, E. J., Nov. 2003. Production regimes in four Eastern  
675 Boundary Current systems. *Deep Sea Research Part II: Topical Studies in*  
676 *Oceanography* 50, 3199–3221.
- 677 Chavez, F. P., Messié, M., 2009. A comparison of eastern boundary upwelling  
678 ecosystems. *Progress in Oceanography* 83 (1-4), 80–96.
- 679 Corten, A., Braham, C.-B., Sadegh, A. S., 2017. The development of a fish-  
680 meal industry in mauritania and its impact on the regional stocks of sar-  
681 dinella and other small pelagics in northwest africa. *Fisheries research* 186,  
682 328–336.
- 683 Corten, A., Mendy, A., Diop, H., 2012. La sardinelle de lafrique du nord-  
684 ouest: Pêches, évaluation des stocks et la gestion. Sub-Regional Fisheries  
685 Commission (SRFC), Dakar.
- 686 Cropper, T. E., Hanna, E., Bigg, G. R., 2014. Spatial and temporal seasonal  
687 trends in coastal upwelling off northwest africa, 1981–2012. *Deep Sea Re-*  
688 *search Part I: Oceanographic Research Papers* 86, 94–111.
- 689 Czaja, A., van der Vaart, P., Marshall, J., Nov. 2002. A Diagnostic Study  
690 of the Role of Remote Forcing in Tropical Atlantic Variability. *Journal of*  
691 *Climate* 15, 3280–3290.
- 692 Di Lorenzo, E., Ohman, M. D., 2013. A double-integration hypothesis to  
693 explain ocean ecosystem response to climate forcing. *Proceedings of the*  
694 *National Academy of Sciences* 110 (7), 2496–2499.  
695 URL <http://www.pnas.org/content/110/7/2496>
- 696 Diankha, O., Thiaw, M., Sow, B. A., Brochier, T., GAYE, A. T., Brehmer,  
697 P., 2015. Round sardinella (*sardinella aurita*) and anchovy (*engraulis en-*  
698 *crasicolus*) abundance as related to temperature in the senegalese waters.  
699 *Thalassas* 31 (2), 9–17.
- 700 Diouf, I., Rodriguez-Fonseca, B., Deme, A., Caminade, C., Morse, A. P.,  
701 Cisse, M., Sy, I., Dia, I., Ermert, V., Ndione, J.-A., et al., 2017. Com-  
702 parison of malaria simulations driven by meteorological observations and

- 703 reanalysis products in senegal. *International journal of environmental re-*  
704 *search and public health* 14 (10), 1119.
- 705 Ebisuzaki, W., Sep. 1997. A Method to Estimate the Statistical Significance  
706 of a Correlation When the Data Are Serially Correlated. *Journal of Climate*  
707 10, 2147–2153.
- 708 Enfield, D. B., Mayer, D. A., Jan. 1997. Tropical Atlantic sea surface tem-  
709 perature variability and its relation to El Niño-Southern Oscillation. 102,  
710 929–945.
- 711 Failler, P., 2014. Climate variability and food security in africa: the case of  
712 small pelagic fish in west africa. *Journal of Fisheries & Livestock Produc-*  
713 *tion* 2 (2), 1–11.
- 714 Frauen, C., Dommenges, D., Tyrrell, N., Rezný, M., Wales, S., 2014. Analysis  
715 of the Nonlinearity of El Niño-Southern Oscillation Teleconnection. 27,  
716 6225.
- 717 Fréon, P., Barange, M., Arístegui, J., Dec. 2009. Eastern Boundary Up-  
718 welling Ecosystems: Integrative and comparative approaches. *Progress in*  
719 *Oceanography* 83, 1–14.
- 720 García-Serrano, J., Cassou, C., Douville, H., Giannini, A., Doblas-Reyes,  
721 F. J., 2017. Revisiting the enso teleconnection to the tropical north at-  
722 lantic. *Journal of Climate* 30 (17), 6945–6957.
- 723 Giannini, A., Chiang, J. C., Cane, M. A., Kushnir, Y., Seager, R., 2001.  
724 The enso teleconnection to the tropical atlantic ocean: Contributions of  
725 the remote and local ssts to rainfall variability in the tropical americas.  
726 *Journal of Climate* 14 (24), 4530–4544.
- 727 Gómez-Letona, M., Ramos, A. G., Coca, J., Arístegui, J., 2017. Trends in  
728 primary production in the canary current upwelling systema regional per-  
729 spective comparing remote sensing models. *Frontiers in Marine Science* 4,  
730 370.
- 731 Ham, Y.-G., Sung, M.-K., An, S.-I., Schubert, S. D., Kug, J.-S., May 2014.  
732 Role of tropical atlantic SST variability as a modulator of El Niño tele-  
733 connections. 50, 247–261.

- 734 King, M. P., Herceg-Bulić, I., Bladé, I., García-Serrano, J., Keenlyside, N.,  
735 Kucharski, F., Li, C., Sobolowski, S., 2018. Importance of late fall enso  
736 teleconnection in the euro-atlantic sector. *Bulletin of the American Mete-*  
737 *orological Society* (2018).
- 738 Lee, S.-K., Enfield, D. B., Wang, C., Aug. 2008. Why do some El Niños have  
739 no impact on tropical North Atlantic SST? *Geophys. Res. Lett.* 35, 16705.
- 740 Lorenz, E. N., 1956. Empirical orthogonal functions and statistical weather  
741 prediction.
- 742 Madec, G., 2008. the nemo team (2008) nemo ocean engine. Note du Pôle de  
743 modélisation. Institut Pierre-Simon Laplace (IPSL), France.
- 744 Marchal, E., 1991. Un essai de caractérisation des populations de poissons  
745 pélagiques côtiers: cas de sardinella aurita des côtes ouest-africaines.
- 746 Meiners, C., Fernández, L., Salmerón, F., Ramos, A., 2010. Climate variabil-  
747 ity and fisheries of black hakes (*merluccius polli* and *merluccius senegalen-*  
748 *sis*) in nw africa: A first approach. *Journal of Marine Systems* 80 (3-4),  
749 243–247.
- 750 Messié, M., Chavez, F. P., 2015. Seasonal regulation of primary production in  
751 eastern boundary upwelling systems. *Progress in Oceanography* 134, 1–18.
- 752 Narayan, N., Paul, A., Mulitza, S., Schulz, M., 2010. Trends in coastal up-  
753 welling intensity during the late 20th century. *Ocean Science* 6 (3), 815.
- 754 Oettli, P., Morioka, Y., Yamagata, T., Jan. 2016. A Regional Climate Mode  
755 Discovered in the North Atlantic: Dakar Niño/Niña. *Scientific Reports* 6,  
756 18782.
- 757 Overland, J. E., Alheit, J., Bakun, A., Hurrell, J. W., Mackas, D. L., Miller,  
758 A. J., 2010. Climate controls on marine ecosystems and fish populations.  
759 *Journal of Marine Systems* 79 (3-4), 305–315.
- 760 Pauly, D., Christensen, V., Mar. 1995. Primary production required to sus-  
761 tain global fisheries. 374, 255–257.
- 762 Polo, I., De Fonseca, B. R., Sheinbaum, J., 2005. Northwest africa upwelling  
763 and the atlantic climate variability. *Geophysical research letters* 32 (23).

- 764 Rayner, N. A., Parker, D. E., Horton, E. B., Folland, C. K., Alexander,  
765 L. V., Rowell, D. P., Kent, E. C., Kaplan, A., Jul. 2003. [DATASET]  
766 Global analyses of sea surface temperature, sea ice, and night marine air  
767 temperature since the late nineteenth century. 108, 4407.
- 768 Roy, C., Reason, C., 2001. ENSO related modulation of coastal upwelling in  
769 the eastern Atlantic. *Progress in Oceanography* 49, 245–255.
- 770 Saha, S., Moorthi, S., Pan, H.-L., Wu, X., Wang, J., Nadiga, S., Tripp, P.,  
771 Kistler, R., Woollen, J., Behringer, D., Liu, H., Stokes, D., Grumbine, R.,  
772 Gayno, G., Wang, J., Hou, Y.-T., Chuang, H.-Y., Juang, H.-M. H., Sela,  
773 J., Iredell, M., Treadon, R., Kleist, D., van Delst, P., Keyser, D., Derber,  
774 J., Ek, M., Meng, J., Wei, H., Yang, R., Lord, S., van den Dool, H., Kumar,  
775 A., Wang, W., Long, C., Chelliah, M., Xue, Y., Huang, B., Schemm, J.-K.,  
776 Ebisuzaki, W., Lin, R., Xie, P., Chen, M., Zhou, S., Higgins, W., Zou, C.-  
777 Z., Liu, Q., Chen, Y., Han, Y., Cucurull, L., Reynolds, R. W., Rutledge,  
778 G., Goldberg, M., Aug. 2010. [DATASET] The NCEP Climate Forecast  
779 System Reanalysis. *Bulletin of the American Meteorological Society* 91,  
780 1015–1057.
- 781 Sánchez-Garrido, J., Werner, F., Fiechter, J., Rose, K., Curchitser, E.,  
782 Ramos, A., Lafuente, J. G., Arístegui, J., Hernández-León, S., San-  
783 tana, A. R., 2019. Decadal-scale variability of sardine and anchovy simu-  
784 lated with an end-to-end coupled model of the canary current ecosystem.  
785 *Progress in Oceanography* 171, 212–230.
- 786 Shchepetkin, A. F., McWilliams, J. C., 2005. The regional oceanic model-  
787 ing system (ROMS): a split-explicit, free-surface, topography-following-  
788 coordinate oceanic model. *Ocean Modelling* 9, 347–404.
- 789 Taschetto, A., Rodrigues, R., Meehl, G., McGregor, S., England, M., 2016.  
790 How sensitive are the pacific–tropical north atlantic teleconnections to the  
791 position and intensity of el niño-related warming? *Climate dynamics* 46 (5-  
792 6), 1841–1860.
- 793 Tsikliras, A. C., Antonopoulou, E., 2006. Reproductive biology of round sar-  
794 dinella (*sardinella aurita*) in north-eastern mediterranean. *Scientia Marina*  
795 70 (2), 281–290.

- 796 Visbeck, M., Chassignet, E. P., Curry, R. G., Delworth, T. L., Dickson, R. R.,  
797 Krahmann, G., 2003. The ocean's response to North Atlantic Oscillation  
798 variability. AGU Geophysical Monograph Series 134, 113–145.
- 799 Wang, C., Feb. 2002. Atmospheric Circulation Cells Associated with the El  
800 Niño-Southern Oscillation. 15, 399–419.
- 801 Wang, C., 2004. ENSO, Atlantic climate variability, and the Walker and  
802 Hadley circulations. In: The Hadley circulation: Present, past and future.  
803 Springer, pp. 173–202.
- 804 Wilks, D. S., 2011. Statistical methods in the atmospheric sciences. Vol. 100.  
805 Academic press.
- 806 Wooster, W. S., Bakun, A., McLain, D. R., 1976. Seasonal upwelling cy-  
807 cle along the eastern boundary of the north atlantic. Journal of Marine  
808 Research 34 (2), 131–141.
- 809 Zeeberg, J., Corten, A., Tjoe-Awie, P., Coca, J., Hamady, B., 2008. Climate  
810 modulates the effects of sardinella aurita fisheries off northwest africa. Fish-  
811 eries Research 89 (1), 65–75.

Supplementary material of the manuscript  
entitled “El Niño as a predictor of round  
sardinella distribution along the northwest  
African coast”

April 1, 2020

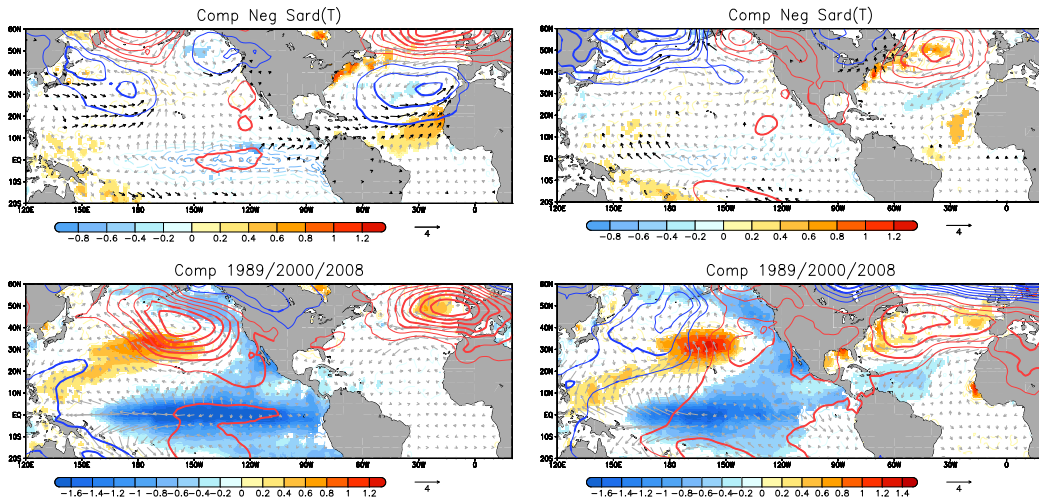


Figure S1: Upper panels: Negative composite maps based on the standardized PC1 (years below -1 standard deviation) of the anomalous round sardinella leading mode. The fields plotted are anomalous SST (shaded the 95% significant response; units in degrees), anomalous SLP (contoured; thick contoured the 95% significant response), and anomalous surface winds (gray vectors; in black the 95% significant response; units in m/s). Bottom panels: the same fields are plotted for La Niña years (years with the Niño 3.4 index below -1 standard deviation). Left panels refer to early winter (Nov-Jan) and right panels to late winter (Feb-Mar).

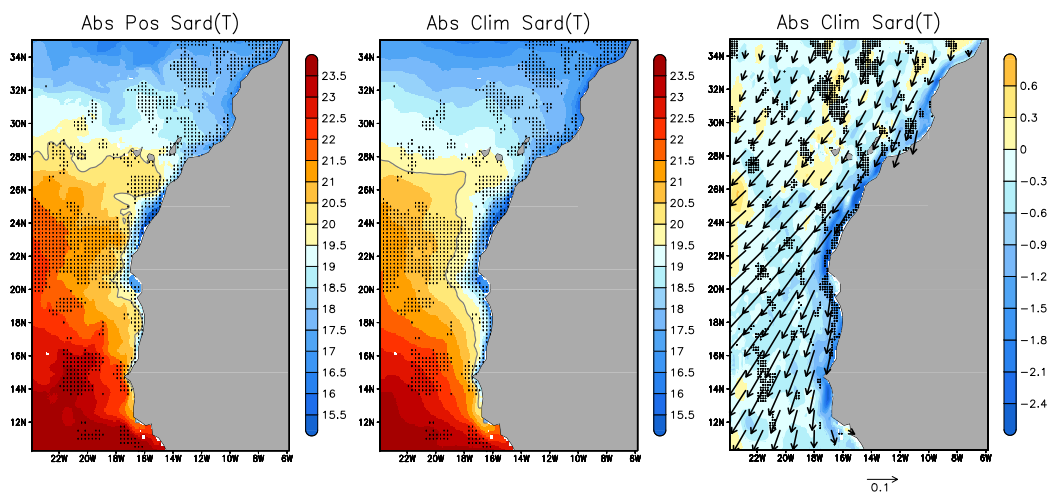


Figure S2: Absolute fields in late winter (Feb-Mar). Temperature of the water column's upper 50 meters under El Niño (left panel) and normal (center panel) conditions. Units in  $^{\circ}\text{C}$ . Black dots represent areas with significant anomalies in Figure 8c). The  $20^{\circ}\text{C}$  isotherm is contoured for a better interpretation. Right panel represents, under normal conditions, the meridional current averaged in the water column's upper 50 meters (shaded; units in  $10 \times \text{m/s}$ ) and the wind stress (vector; units in  $\text{N/m}^2$ ). Black dots highlight areas with positive significant anomalies in Figure 8d.

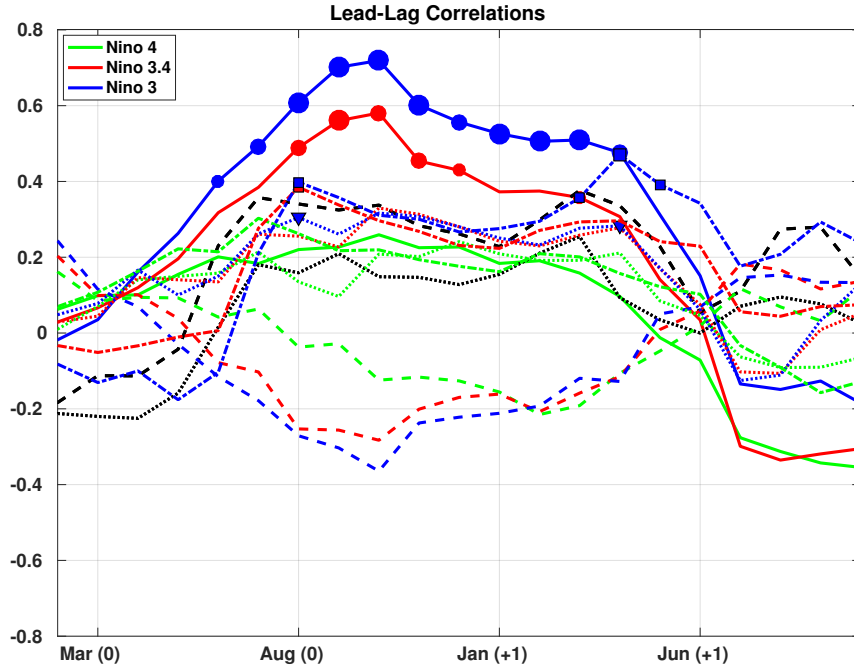


Figure S3: In solid lines the linear correlation coefficients between the leading sardinella mode (i.e., the corresponding PC) in JFM (year +1; see Figure 6a) and the Niño 3 (blue), Niño 4 (green), and Niño 3.4 (red) indices at different time lags. The same is shown for: 1) the meridional current of the water column's upper 50 meters off Cape Blanc in early (dashed lines) and late (dotted lines) winter, and 2) the temperature of the water column's upper 50 meters off Cape Blanc in late winter (dashed-pointed lines). The region off Cape Blanc is defined as the area within the red square indicated in Figure 8. Small, medium and large size of symbols (dots, squares and triangles) represent correlations at the 99%, 95% and 90% confidence level respectively according to the non-parametric test described by Ebisuzaki et al., 2017. Finally, black dashed (dotted) line shows the correlation between the leading sardinella mode and the zonal (meridional) wind stress averaged within the green boxes indicated in Figure 8.

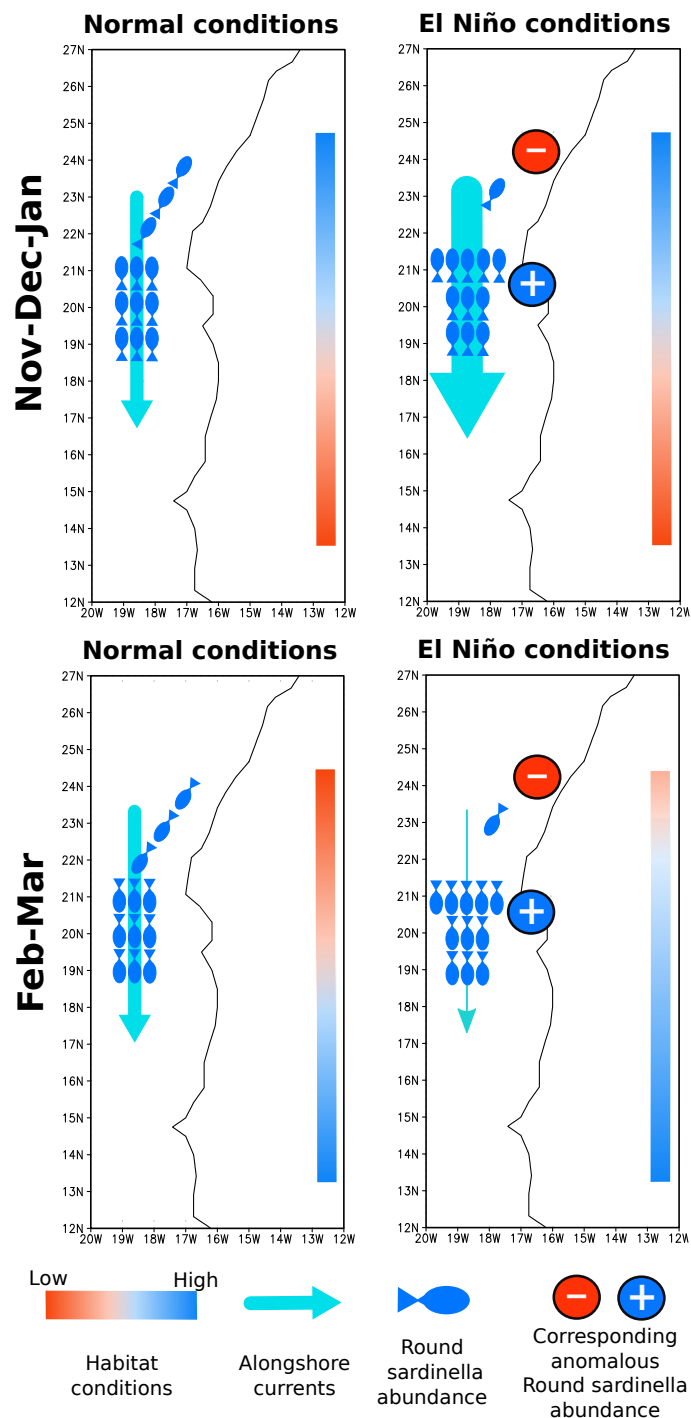


Figure S4: **Simplified representation of the round sardinella response to El Niño.** Upper panels corresponds to early winter and bottom panels to late winter. Left panels correspond to normal conditions and right panels to El Niño influenced conditions. Illustrated the absolute round sardinella biomass, the anomalous biomass response to El Niño, the alongshore currents, and the meridional evolution of the<sup>5</sup> habitat quality of round sardinella (depending on water temperature and food abundance in the water column's upper 50 meters) along the African coast.

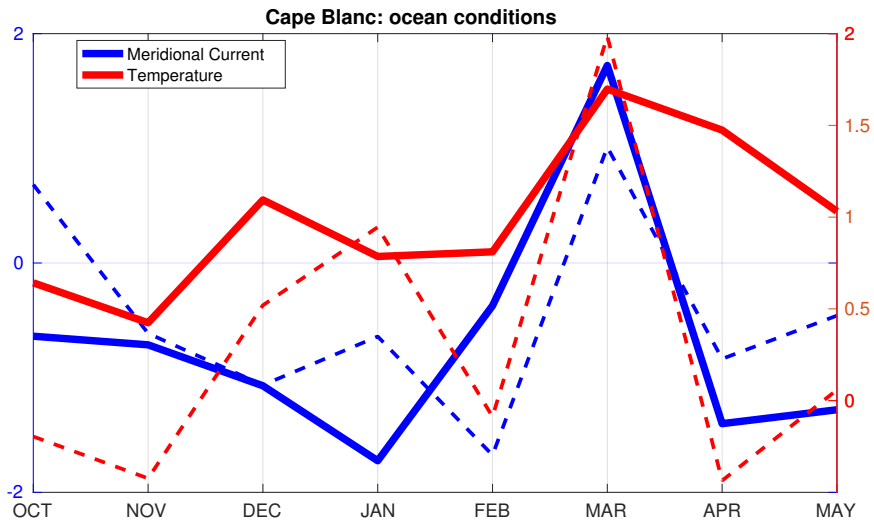


Figure S5: In solid line the averaged evolution, during El Niño years and off Cape Blanc, of the observed sea surface temperature (from the NOAA GHRSSST V.2; [https://podaac.jpl.nasa.gov/dataset/AVHRR\\_OI-NCEI-L4-GLOB-v2.0](https://podaac.jpl.nasa.gov/dataset/AVHRR_OI-NCEI-L4-GLOB-v2.0)) and the observed surface meridional current (from OSCAR third degree resolution ocean surface currents; [https://podaac.jpl.nasa.gov/dataset/OSCAR\\_L4\\_OC\\_third-deg](https://podaac.jpl.nasa.gov/dataset/OSCAR_L4_OC_third-deg)). In dashed line the same evolution is shown for the modeled (ROMS-PISCES) water temperature and meridional current averaged in the water column's upper 50 meters off Cape Blanc. In all cases the standardized monthly means are calculated in the area within the red square indicated in Figure 8.